

# One-Step Semisynthesis of a Segetane Diterpenoid from a Jatrophane Precursor via a Diels–Alder Reaction

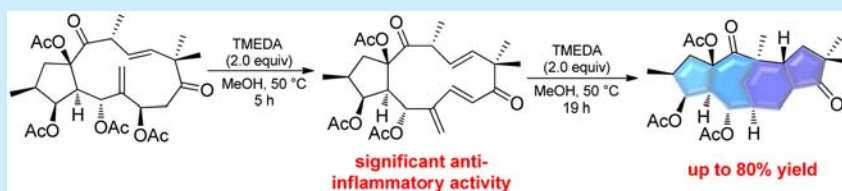
Luo-Sheng Wan,<sup>†</sup> Li-Dong Shao,<sup>†</sup> Liangbing Fu,<sup>‡</sup> Jun Xu,<sup>†,§</sup> Guo-Lei Zhu,<sup>†,§</sup> Xing-Rong Peng,<sup>†</sup> Xiao-Nian Li,<sup>†</sup> Yan Li,<sup>†</sup> and Ming-Hua Qiu<sup>\*,†,§</sup>

<sup>†</sup>State Key Laboratory of Phytochemistry and Plant Resources in West China, Kunming Institute of Botany, Chinese Academy of Sciences, 132 Lanhei Road, Kunming 650201, P. R. China

<sup>‡</sup>Department of Chemistry, Emory University, 1515 Dickey Drive, Atlanta, Georgia 30322, United States

<sup>§</sup>University of Chinese Academy of Sciences, Beijing 100049, P. R. China

## S Supporting Information



**ABSTRACT:** A novel segetane diterpenoid (**1**) and four jatrophane diterpenoids (**2–5**) were isolated from an acetone extract of *Euphorbia peplus*. Due to quantity limitations, we prepared **1** via a Diels–Alder reaction, an approach motivated by this compound's biosynthetic pathway and successfully performed X-ray analysis of **1**. Furthermore, in an *in vitro* activity test, **1** exhibited moderate anti-inflammatory activity, whereas both its precursor (**2**) and the relevant intermediate (**2a**, IC<sub>50</sub> = 1.56 μM) exhibited significant anti-inflammatory activity.

Plants in the genus *Euphorbia* are well-known for possessing diterpenoids with diverse, complex skeletons and a broad spectrum of therapeutically relevant biological activities (including therapeutic effects for skin diseases as well as anti-inflammatory, antimicrobial, cytotoxic, and multidrug resistance-reversing activities).<sup>1</sup> One of the most intriguing of these diterpenoids, ingenol mebutate from *E. peplus*, has been approved by the FDA and the EMA for the treatment of actinic keratosis, which can transform into squamous cell carcinoma.<sup>2</sup> Moreover, the entire *E. peplus* plant is used in traditional medicine to treat inflammation, asthma, and tumors.<sup>3</sup> In addition to ingenol mebutate, *E. peplus* contains other interesting components, such as pepluane<sup>4</sup> and jatrophane<sup>5</sup> diterpenoids, which have inspired researchers to focus on these compounds' anti-inflammatory<sup>6</sup> and multidrug resistance-reversing<sup>7</sup> activities.

To date, although numerous ingenane and jatrophane diterpenoids have been obtained from *E. segetalis*, *E. portlandica*, and *E. paralias*, only 10 segetane diterpenoids have been isolated from these plants, despite the fact that segetane diterpenoids have fascinating activities.<sup>7b,8</sup> To discover more segetane diterpenoids, we examined *E. peplus*, which has certain structures that are biogenetically related to those of *E. paralias*;<sup>6</sup> using this approach, we identified a novel segetane diterpenoid (**1**) and four jatrophane diterpenoids (**2–5**) (Figure 1). However, due to the overlapping signals of CH<sub>3</sub>-18 and CH<sub>3</sub>-19, the orientation of H-12 in **1** could not readily be determined using only ROESY correlations without X-ray diffraction analysis. After analyzing the biosynthesis of **1**, we prepared this compound from a precursor (**2**, 20 mg) in a single step via a Diels–Alder reaction,

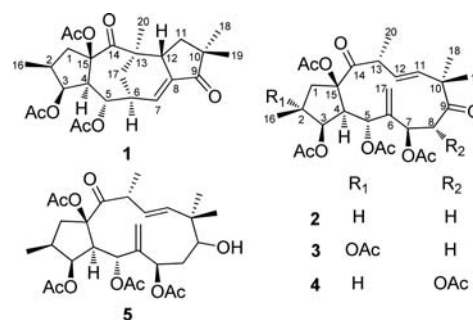


Figure 1. Structures of **1–5**.

successfully obtained a prismatic crystal from 16 mg of product, and performed X-ray diffraction crystallography. Moreover, the generalized version of this reaction was subjected to preliminary analysis.

Anti-inflammatory assays revealed that in contrast to **1**, **1**'s precursor (**2**) and the relevant intermediate (**2a**) exhibited exceptionally potent NO production activities in an LPS-stimulated RAW264.7 cell model. The most potent compound, which was the intermediate (**2a**), is approximately 54 times as active as **1**, revealing the presence of a structure–activity relationship (SAR).

Received: December 14, 2015

Published: January 19, 2016

Here, we present the isolation, structural elucidation, and anti-inflammatory activities of **1–5** (including two reaction products, **2a** and **3a**) as well as the bioinspired semisynthesis of **1**.

The molecular formula of **1**,  $C_{26}H_{34}O_8$ , which includes ten degrees of unsaturation, was determined from this compound's HRESIMS spectrum, which featured an  $m/z$  of 497.2151 (calcd. for  $C_{26}H_{34}O_8Na$ , 497.2151); this formula was supported by NMR data (Table 1). In the  $^1H$  and  $^{13}C$  NMR spectra of **1**, the

Table 1. NMR Data for **1** and **2a**<sup>a</sup>

	<b>1</b>		<b>2a</b>	
	$\delta_H$	$\delta_C$ , type	$\delta_H$	$\delta_C$ , type
1 $\alpha$	3.55 dd (14.6, 8.3)	43.6, CH <sub>2</sub>	2.68 dd (13.5, 7.3)	44.5, CH <sub>2</sub>
1 $\beta$	1.40 m		1.74 m	
2	2.06 m	37.4, CH	2.33 m	36.0, CH
3	5.38 brs	77.5, CH	5.40 t (5.4)	75.2, CH
4	2.26 dd (10.6, 3.4)	52.1, CH	2.71 dd (5.4, 3.1)	51.4, CH
5	5.29 d (10.6)	68.6, CH	5.98 d (3.1)	70.0, CH
6	2.77 t (6.4)	39.6, CH		143.5, C
7	6.99 d (7.0)	131.1, CH	6.73 d (16.3)	136.3, CH
8		142.8, C	6.64 d (16.3)	129.7, CH
9		209.1, C		202.3, C
10		44.9, C		49.4, C
11	1.36 t (12.0)	39.9, CH <sub>2</sub>	5.64 d (16.0)	138.8, CH
	1.80 dd (11.1, 6.2)			
12	2.65 m	36.8, CH	5.46 dd (16.0, 8.0)	130.7, CH
13		48.0, C	3.61 m	44.5, CH
14		204.2, C		210.5, C
15		91.6, C		91.4, C
16	0.92 d (6.6)	13.6, CH <sub>3</sub>	0.93 d (6.9)	13.5, CH <sub>3</sub>
17	1.44 m; 1.94 m	30.5, CH <sub>2</sub>	5.35 brs	118.8, CH <sub>2</sub>
18	1.07 s	24.2, CH <sub>3</sub>	1.22 s	22.8, CH <sub>3</sub>
19	1.09 s	24.6, CH <sub>3</sub>	1.27 s	24.0, CH <sub>3</sub>
20	1.24 s	22.7, CH <sub>3</sub>	1.16 d (6.7)	18.2, CH <sub>3</sub>
3-OAc	2.04 s	169.7, C	2.16 s	170.1, C
		20.6, CH <sub>3</sub>		20.9, CH <sub>3</sub>
5-OAc	2.05 s	169.9, C	2.13 s	169.3, C
		21.1, CH <sub>3</sub>		21.3, CH <sub>3</sub>
15-OAc	1.88 s	171.2, C	2.05 s	170.1, C
		21.7, CH <sub>3</sub>		21.5, CH <sub>3</sub>

<sup>a</sup>NMR data ( $\delta$ ) were obtained at 600 and 150 MHz for  $^1H$  and  $^{13}C$ , respectively, in  $CDCl_3$ . Proton coupling constants ( $J$ ) in Hz are provided in parentheses.

presence of three acetates was easily deduced from their typical signals. The remaining 20  $^{13}C$  DEPT signals were attributed to four methyls (one secondary and three tertiary methyls, as determined by  $^1H$  NMR), three methylenes, seven methines (one olefinic methine and two oxygenated methines), and six quaternary carbons (two tetrasubstituted carbons, two carbonyl carbons, one olefinic carbon, and one oxygenated carbon); these assignments are consistent with the functional units observed in  $^1H$  NMR and HSQC spectra. In combination with correlations detected in  $^1H$ – $^1H$  ROESY (Figure 2a), these spectroscopic data indicate that **1** is a segetane diterpenoid with three acetyloxy groups at C-3, C-5, and C-15. In addition, the locations of two carbonyl groups were further supported by HMBC spectroscopic analysis (Figure 2a).

Specifically, diagnostic correlations from the olefinic proton H-7 and H<sub>3</sub>-18 to a carbon at  $\delta_C$  209.1 suggested that one carbonyl group was located at C-9. Furthermore, the location of the other carbonyl at C-14 was deduced from the correlations of

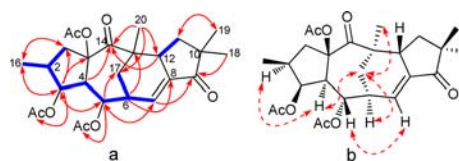


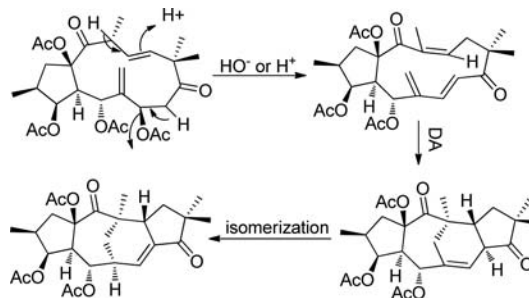
Figure 2. (a) Key  $^1H$ – $^1H$  COSY (thick blue lines) and three-bond HMBC correlations (red arrows from  $^1H$  to  $^{13}C$ ) for **1**. (b) Main ROESY enhancements (red dashed lines with double arrows) for **1**.

H-4, H-12, and H<sub>3</sub>-20 with a carbon at  $\delta_C$  204.2. Thus, the planar structure of **1** depicted below was determined.

The partial relative configuration of **1** was drawn based on interpretations of ROESY cross-peaks (Figure 2b). The H-2/H-4, H-4/H<sub>2</sub>-17, H<sub>2</sub>-17/H<sub>3</sub>-20, H<sub>2</sub>-17/H-6, and H-5/H-7 ROESY correlations indicated that H<sub>2</sub>-17 is near H-4 and that the bridge configuration and H-2 are in the  $\alpha$ -orientation. However, there were no useful correlations involving the overlapping signals of H<sub>3</sub>-18 and H<sub>3</sub>-19 to support conclusions regarding the orientation of H-12. After many attempts, we failed to obtain a crystal for X-ray diffraction analysis due to the limited quantity of **1** that was isolated (0.9 mg).

When analyzing the biosynthesis of **1**, we found that **2** might be a precursor of **1** via a Diels–Alder reaction in the presence of a Lewis base and/or a Lewis acid (Scheme 1), unlike the

Scheme 1. Plausible Biosynthetic Pathway of **1**



biosynthesis proposed by Barile et al. that the segetane tetracyclic skeleton was formed by a two-steps cyclization of jatrophane derivative.<sup>8a</sup> Thus, we conducted this reaction, using 2.0 equiv of  $N,N,N',N'$ -tetramethyl-ethylenediamine (TMEDA) as the catalyst<sup>10</sup> and methanol as the solvent at 50 °C. As indicated in Scheme 2, after the reaction had proceeded for 5 h, 90% yield of the intermediate **2a** (Table 1) was obtained. After the reaction proceeded for another 19 h, the intermediate **2a** had disappeared, and the final product **1** had appeared, with a yield of 90%. Given the sufficient quantity of **1** obtained in this reaction, we successfully determined the X-ray crystal structure of **1** (Figure 3),<sup>11</sup> which is identical to the structure obtained from NMR data (Supporting Information) and has parallel optical rotation with the structure determined from previously isolated product. We confirmed that H-12 in **1** is in the  $\beta$ -orientation, which represents a novel configuration opposite from previously reported configurations.<sup>8</sup>

To clarify the general nature of the aforementioned reaction, we used **3**, which differs from **2** only at C-2 (Scheme 2), as the reactant under identical conditions. After reacting for 24 h, **3** produced a final product **3a** with a skeleton identical to that of **1**. However, when we used **4** and **5**, which differ from **2** only at C-8 (an acetyloxy group in **4**) and C-9 (a hydroxy group in **5**), respectively, only certain hydrolysates were produced after the

Scheme 2. Reaction Process and Its Crucial Points

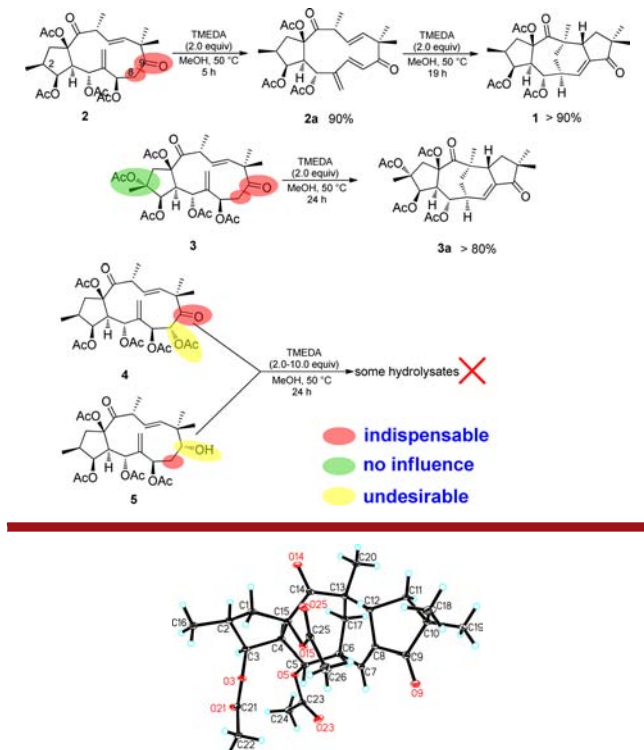


Figure 3. X-ray crystallographic structure of 1.

reaction proceeded for 24 h, even when 10.0 equiv of TMEDA was used as the catalyst. Based on these results, the proposed biosynthetic pathway of **1** was proven. Through an elimination reaction, **2** could be converted to the intermediate **2a**, which could be transformed into **1** via a Diels–Alder reaction. The partially stereospecific formation of **1** can be interpreted based on the stereochemistry of **2**, which has an  $\alpha$ -H at C-2 and C-4, an  $\alpha$ -CH<sub>3</sub> at C-13, and a  $\beta$ -acetoxy group at C-15. In addition, the preliminary study of the generalization of this reaction revealed that a carbonyl at C-9 and a lack of substitution at C-8 are indispensable to the formation of a segetane skeleton from a jatrophone skeleton.

Nitric oxide synthase (iNOS) isoform, which is an essential enzyme in host innate immunity and inflammation that is relevant to various pathogens, can induce the production of NO free radicals.<sup>12</sup> Considering the traditional use of *E. peplus*, all of the aforementioned compounds (**1**–**5**, **2a**, and **3a**) were tested to determine their inhibitory activities against NO production in an LPS-stimulated RAW264.7 cell model. The intermediate **2a** exhibited strong inhibitory activity against NO production; in particular, with respect to such activity, **2a** was 7, 54, and 58 times more potent than **2**, **1**, and **3a**, respectively (Table 2). The

Table 2. Inhibitory Effects on LPS-Stimulated NO Production in RAW264.7 Cells

compd	IC <sub>50</sub> ( $\mu$ M)	compd	IC <sub>50</sub> ( $\mu$ M)
<b>1</b>	84.36	<b>3</b>	81.13
<b>2a</b>	1.56	<b>4</b>	>100
<b>2</b>	11.76	<b>5</b>	>100
<b>3a</b>	91.34	MG-132 <sup>b</sup>	0.18

<sup>b</sup>Positive control.

viability of RAW 264.7 cells was determined to exclude interference that could affect cytotoxicity. Based on the MTT assay, none of the compounds at any of the tested concentrations exhibited obvious cytotoxicity to RAW264.7 cells.

In conclusion, we have determined a one-step, efficient, bioinspired semisynthesis for the formation of segetane skeletons (**1**, **3a**) from jatrophone skeletons. X-ray diffraction analysis proved that **1** is a natural segetane diterpenoid with a novel  $\beta$ -oriented H-12. Moreover, given the significantly enhanced anti-inflammatory activity of the intermediate **2a**, this molecule is a promising initial compound for further SAR investigations.

## ■ ASSOCIATED CONTENT

### Supporting Information

The Supporting Information is available free of charge on the ACS Publications website at DOI: 10.1021/acs.orglett.5b03473.

X-ray data for compound **1** (CIF)

Experimental section, X-ray crystallographic data of **1**, spectroscopic spectra of compound **1**–**5**, **2a**, and **3a** (PDF)

## ■ AUTHOR INFORMATION

### Corresponding Author

\*E-mail: mhchiu@mail.kib.ac.cn.

### Notes

The authors declare no competing financial interest.

## ■ ACKNOWLEDGMENTS

The project was financially supported by the Youth Program of National Natural Science Foundation of China (NSFC, No. 81403050) and Joint Foundation of NSFC and Natural Science Foundation of Yunnan (NSFY, No. U1132604). The authors were particularly grateful to Senior Engineer Jian-Chao Chen from the Kunming Institute of Botany, Chinese Academy of Sciences, for the assistance with NMR analysis.

## ■ REFERENCES

- (1) (a) Wang, H. B.; Wang, X. Y.; Liu, L. P.; Qin, G. W.; Kang, T. G. *Chem. Rev.* **2015**, *115*, 2975–3011. (b) Vasas, A.; Hohmann, J. *Chem. Rev.* **2014**, *114*, 8579–8612. (c) Shi, Q. W.; Su, X. H.; Kiyota, H. *Chem. Rev.* **2008**, *108*, 4295–4327.
- (2) Keating, G. M. *Drugs* **2012**, *72*, 2397–2405.
- (3) An Editorial Committee of the Flora of China. *Flora of China*; Science Press: Beijing, 1990; Vol. 44, p 111.
- (4) Corea, G.; Fattorusso, E.; Lanzotti, V.; Di Meglio, P.; Maffia, P.; Grassia, G.; Ialenti, A.; Ianaro, A. *J. Med. Chem.* **2005**, *48*, 7055–7062.
- (5) (a) Corea, G.; Fattorusso, E.; Lanzotti, V.; Motti, R.; Simon, P. N.; Dumontet, C.; Di Pietro, A. *J. Med. Chem.* **2004**, *47*, 988–992. (b) Corea, G.; Fattorusso, E.; Lanzotti, V.; Tagliatela-Scafati, O.; Appendino, G.; Ballero, M.; Simon, P. N.; Dumontet, C.; Di Pietro, A. *J. Med. Chem.* **2003**, *46*, 3395–3402.
- (6) Barile, E.; Fattorusso, E.; Ialenti, A.; Ianaro, A.; Lanzotti, V. *Bioorg. Med. Chem. Lett.* **2007**, *17*, 4196–4200.
- (7) (a) Jadranin, M.; Pesic, M.; Aljancic, I. S.; Milosavljevic, S. M.; Todorovic, N. M.; Podolski-Renic, A.; Bankovic, J.; Tanic, N.; Markovic, I.; Vajs, V. E.; Tesevic, V. V. *Phytochemistry* **2013**, *86*, 208–217. (b) Sousa, I. J.; Ferreira, M. J.; Molnar, J.; Fernandes, M. X. *Eur. J. Pharm. Sci.* **2013**, *48*, 542–553. (c) Valente, I.; Reis, M.; Duarte, N.; Serly, J.; Molnar, J.; Ferreira, M. J. *J. Nat. Prod.* **2012**, *75*, 1915–1921. (d) Aljancic, I. S.; Pesic, M.; Milosavljevic, S. M.; Todorovic, N. M.; Jadranin, M.; Milosavljevic, G.; Povrenovic, D.; Bankovic, J.; Tanic, N.; Markovic, I. D.; Ruzdijic, S.; Vajs, V. E.; Tesevic, V. V. *J. Nat. Prod.* **2011**, *74*, 1613–

1620. (e) Vasas, A.; Sulyok, E.; Redei, D.; Forgo, P.; Szabo, P.; Zupko, I.; Berenyi, A.; Molnar, J.; Hohmann, J. *J. Nat. Prod.* **2011**, *74*, 1453–1461.
- (8) (a) Barile, E.; Lanzotti, V. *Org. Lett.* **2007**, *9*, 3603–3606. (b) Abdelgaleil, S. A.; el-Aswad, A. F.; Nakatani, M. *Pest Manage. Sci.* **2002**, *58*, 479–482. (c) Abdelgaleil, S. A.; Kassem, S. M.; Doe, M.; Baba, M.; Nakatani, M. *Phytochemistry* **2001**, *58*, 1135–1139. (d) Jakupovic, J.; Morgenstern, T.; Marco, J. A.; Berendsohn, W. *Phytochemistry* **1998**, *47*, 1611–1619. (e) Jakupovic, J.; Jeske, F.; Morgenstern, T.; Tschritzis, F.; Marco, J. A.; Berendsohn, W. *Phytochemistry* **1998**, *47*, 1583–1600. (f) Oksuz, S.; Gurek, F.; Yang, S. W.; Lin, L. Z.; Cordell, G. A.; Pezzuto, J. M.; Wagner, H.; Lotter, H. *Tetrahedron* **1997**, *53*, 3215–3222.
- (9) Compound (**1**): colorless prismatic crystal,  $[\alpha]_D^{25}$  58.6 (0.23, MeOH); UV (MeOH)  $\lambda_{\max}$  (log  $\epsilon$ ) 242 (3.82) nm; IR (KBr)  $\nu_{\max}$  2926, 1734, 1656, 1458, 1381, 1246, 1139, 1031  $\text{cm}^{-1}$ ;  $^1\text{H}$  NMR ( $\text{CDCl}_3$ , 600 MHz) data, see Table 1;  $^{13}\text{C}$  NMR ( $\text{CDCl}_3$ , 150 MHz) data, see Table 1; (+)HRESIMS  $m/z$   $[\text{M} + \text{Na}]^+$  497.2151 (calcd for  $\text{C}_{26}\text{H}_{34}\text{O}_8\text{Na}$ , 497.2151). For plant material, isolation procedures, and 1D and 2D NMR spectra, see Supporting Information.
- (10) Li, X. Y.; Yang, Y. F.; Peng, X. R.; Li, M. M.; Li, L. Q.; Deng, X.; Qin, H. B.; Liu, J. Q.; Qiu, M. H. *Org. Lett.* **2014**, *16*, 2196–2199.
- (11) Crystallographic data of compound (**1**) have been deposited at the Cambridge Crystallographic Data Centre (deposition no. CCDC 1440725). Copies of the data can be obtained free of charge via [www.ccdc.cam.ac.uk](http://www.ccdc.cam.ac.uk).
- (12) McCartney-Francis, N. L.; Song, X.; Mizel, D. E.; Wahl, S. M. *J. Immunol.* **2001**, *166*, 2734–2740.